Molecular Biology of the Cell
Vol. 12, 589–599, March 2001

# Polaris, a Protein Involved in Left-Right Axis Patterning, Localizes to Basal Bodies and Cilia

**Patrick D. Taulman,* Courtney J. Haycraft,* Daniel F. Balkovetz,*†‡ and Bradley K. Yoder*§**

*Department of Cell Biology, University of Alabama at Birmingham, Birmingham, Alabama 35294; †Department of Medicine, University of Alabama at Birmingham, Birmingham, Alabama 35294; and ‡Birmingham Veterans Affairs Medical Center, Birmingham, Alabama 35294

Submitted August 8, 2000; Revised November 30, 2000; Accepted January 9, 2000
Monitoring Editor: John C. Gerhart

Mutations in *Tg737* cause a wide spectrum of phenotypes, including random left-right axis specification, polycystic kidney disease, liver and pancreatic defects, hydrocephalus, and skeletal patterning abnormalities. To further assess the biological function of *Tg737* and its role in the mutant pathology, we identified the cell population expressing *Tg737* and determined the subcellular localization of its protein product called Polaris. *Tg737* expression is associated with cells possessing either motile or immotile cilia and sperm. Similarly, Polaris concentrated just below the apical membrane in the region of the basal bodies and within the cilia or flagellar axoneme. The data suggest that Polaris functions in a ciliogenic pathway or in cilia maintenance, a role supported by the loss of cilia on the ependymal cell layer in ventricles of $Tg737^{orpk}$ brains and by the lack of node cilia in $Tg737^{\Delta 2\text{-}3\beta Gal}$ mutants.

## INTRODUCTION

Many cells rely on cilia for proper function (Wheatley *et al.*, 1996). In vertebrates, there are immotile cilia, in which receptors are concentrated to survey the local environment, and motile cilia, which are involved in fluid movement (Satir and Sleigh, 1990; Handel *et al.*, 1999). Basal bodies in the apical cytoplasm initiate cilium formation during which proteins involved in ciliogenesis concentrate and assemble into complexes that migrate up the cilia axoneme as large rafts, a process called intraflagellar transport (IFT) (Kozminski *et al.*, 1993; Cole *et al.*, 1998). Mutations that block IFT have severe consequences to the organisms, resulting from ciliary dysfunction.

In addition to sensory reception and fluid movement, cilia are also thought to function in patterning of the left-right (LR) body axis (Nonaka *et al.*, 1998). The connection between LR axis specification and cilia is supported by the LR defects seen in several murine mutations (*Kif3A, Kif3B*, and *lrd*) that disrupt node cilia formation or motility and from the situs inversus observed in human Kartagener's patients where cilia are immotile (Afzelius, 1976; Supp *et al.*, 1997; Nonaka *et al.*, 1998; Marszalek *et al.*, 1999; Takeda *et al.*, 1999). Hirokawa and colleagues recently proposed the "nodal flow" hypothesis (Nonaka *et al.*, 1998; Okada *et al.*, 1999). According to this model, cilia on the embryonic node create a leftward current in the extraembryonic fluid that establishes an asymmetric gradient of a LR morphogen. Although there is a strong correlation between ciliary function and LR patterning, the nodal flow hypothesis cannot adequately explain the consistent LR reversal seen in the mouse inversion of embryonic turning (*inv*) mutant, where node cilia are present and the leftward flow is maintained (Yokoyama *et al.*, 1993; Okada *et al.*, 1999; Wagner and Yost, 2000). Furthermore, many of the genes implicated in LR specification are also expressed in nonciliated cells where they have other functions. Thus, to further evaluate the relevancy of cilia and the nodal flow hypothesis to LR axis determination, it is important to fully elucidate the function of the proteins known to affect axis determination.

In this regard, a new allele ($Tg737^{\Delta 2\text{-}3\beta Gal}$) of the *TgN737Rpw* (*Tg737*) gene was recently described where the LR axis is randomly determined (Murcia *et al.*, 2000). Similar to the *Kif3A* and *Kif3B* mutants, $Tg737^{\Delta 2\text{-}3\beta Gal}$ mice die during early to mid-gestation, have abnormal midline development, and lack node cilia. *Tg737* was first identified through its association with the hypomorphic allele in the Oak Ridge polycystic kidney ($Tg737^{orpk}$) mouse (Moyer *et al.*, 1994). In contrast to the severe embryonic defects in $Tg737^{\Delta 2\text{-}3\beta Gal}$ mutants, $Tg737^{orpk}$ mice survive into young adulthood and exhibit a complex phenotype, including cystic kidneys, liver and pancreatic defects, and skeletal patterning abnormalities. Here we further characterize *Tg737* by identifying the cells in which it functions and by determining the subcellular localization of Polaris, the tetratricopeptide repeat (TPR) containing protein encoded by *Tg737*. Although previous Northern analysis suggests that *Tg737* is ubiquitously ex-

§ Corresponding author. E-mail address: Byoder@uab.edu.

pressed as multiple spliced transcripts, spatial analysis described in this report indicates that *Tg737* expression is concentrated in ciliated epithelium and that Polaris is localized to the basal bodies and within the cilium axoneme (Moyer *et al.*, 1994; Yoder *et al.*, 1995). In agreement with this localization, cilia are aberrantly formed on the ependymal cells lining the ventricles in the $Tg737^{orpk}$ brain and are completely abolished on the embryonic node of $Tg737^{\Delta 2\text{-}3\beta Gal}$ mutants. Together, the spatial expression analysis, the immunolocalization data, and the phenotypes of mice with mutations in *Tg737* suggest that Polaris functions in a ciliogenic pathway.

## MATERIALS AND METHODS

### *Antibodies*

Antisera against Polaris were generated in four rabbits by using a 21-residue peptide (NVHLAPETDEDDLYSGFNDYN) starting at position 3 of the mouse protein according to the standard protocol established by Genosys Biotechnologies (The Woodlands, TX). Enzyme-linked immunosorbent assay was used to evaluate the antibody titer, and affinity-purified sera (Genosys) from three rabbits (GN593, GN1439, and GN1440) were used for subsequent analyses. Specificity of the antisera against Polaris was confirmed by Western blot analysis of protein extracts isolated from $Tg737^{orpk}$ and $Tg737^{\Delta 2\text{-}3\beta Gal}$ mice and by immunoprecipitation of in vitro translated Polaris protein. The antisera specificity for Polaris is further demonstrated by the correlation of the $\beta$-galactosidase staining pattern and intensity with the immunofluorescence localization of the protein.

### *Immunolocalization*

Tissues were isolated from wild-type mice, embedded in Tissue-Tek O.C.T. compound (Sakura Finetek U.S.A., Inc., Torrance, CA.), cut into 5-$\mu$m sections and fixed for 10 min with 4% formaldehyde, 0.2% Triton X-100 in phosphate-buffered saline (PBS). Sections were incubated in blocking buffer (1% bovine serum albumin in PBS) for 10 min, followed by a 45-min incubation with primary antibody diluted in blocking buffer. After three washes in PBS, slides were incubated for 45 min in secondary antibody (Jackson ImmunoResearch, West Grove, PA) diluted in blocking buffer. Nuclei were stained using Hoechst No. 33528 (Sigma, St. Louis, MO) diluted 1:1000 in PBS, and coverslips attached. Immunofluorescent labeling of polarized Madin-Darby canine kidney (MDCK) cells grown on filters was performed as previously described (Balkovetz *et al.*, 1997). Identical results were obtained with all three sera.

### *Western Blotting*

Tissues or embryos (embryonic day 8.0) were isolated and dounce homogenized in BOD (1% NP-40, 1% Triton X-100, 1% SDS in PBS). Protein concentration was determined using the $D_C$ protein assay kit as described by the manufacturer (Bio-Rad, Richmond, CA). Thirty micrograms of each protein lysate was resolved by electrophoresis on a 10% SDS-PAGE gel and the proteins transferred to nitrocellulose (NitroBind; Micron Separations, Westboro, MA). Filters were blocked in 5% dry milk/PBS and Western blot analysis was conducted using affinity-purified anti-Polaris antibodies (dilution of 1:1000) and horseradish peroxidase-conjugated anti-rabbit secondary antibodies (diluted 1:5000; Bio-Rad). The horseradish peroxidase signal was detected using Supersignal West Femto Chemiluminescence kit (Pierce, Rockford, IL).

### *$\beta$-Galactosidase Assays*

For $\beta$-galactosidase assays, tissues were isolated from $Tg737^{\Delta 2\text{-}3\beta Gal}$ heterozygous and wild-type mice. Tissues were fixed in 2% paraformaldehyde/PBS for 2 to 4 h, washed in PBS, infiltrated with 30% sucrose in PBS for 24 h, and snap frozen in OCT freezing compound. Five-micron sections were cut with a Leica CM1900 cryostat and sections were attached to Probe-On charged slides. After postfixation in 0.2% paraformaldehyde in 0.1 M piperazine-*N*,*N*′-bis(2-ethanesulfonic acid) pH 6.5 and permeabilization in 0.05% NP-40/PBS for 15 min, slides were washed once in PBS containing 2 mM $MgCl_2$ and incubated in X-Gal staining solution (2 mM $MgCl_2$, 5 mM potassium ferrocyanide, 5 mM potassium ferricyanide, 1 mg $ml^{-1}$ X-Gal, 1× PBS) at 37°C for 2 to 24 h. Sections were counterstained with nuclear fast red as described by the manufacturer (Vector Laboratories, Burlingame, CA) and coverslips were attached using Permount. The specificity of the $\beta$-galactosidase reporter gene assay was demonstrated by its good correlation with immunolocalization data. Images were captured using a Coolpix 900 digital camera attached to a Nikon TE200 inverted microscope or a Nikon SMZ800 stereomicroscope. No $\beta$-galactosidase activity was detected in sections derived from wild-type mice.

### *Northern Blot Analysis*

Total RNA was isolated from adult wild-type, $Tg737^{orpk}$ heterozygous, and $Tg737^{orpk}$ homozygous mice by using the guanidinium isothiocyanate/cesium chloride cushion procedure and enriched for polyadenylated RNA by passage over oligo-dT columns. Two micrograms of Poly($A^+$) RNA was resolved by denaturing agarose gel electrophoresis, transferred to charged nitrocellulose membranes, and hybridized with the *Tg737* cDNA that was labeled with $\alpha$-$^{32}$P-deoxycytidine 5′-triphosphate by using the random hexamer method (Sambrook *et al.*, 1989).

### *Cell Culture and Transfection*

The isolation and characterization of the mutant BroF2 liver cell line was described previously (Richards *et al.*, 1997; Yoder *et al.*, 1997). The 94D renal cell line was isolated by microdissection of cortical collecting duct segments from *orpk* mutant mice on the Immorto-Mouse (Charles River Laboratory, Wilmington, MA) background. Individual cell suspensions from small segments of collecting tubules were generated by dilute collagenase treatment (0.1 g $dl^{-1}$ collagenase II, 5 mM glycine, 50 U $ml^{-1}$ DNase, in minimal essential medium). A clonal cell line (94D) was propagated from a single dissected tubule on collagen-treated culture vessels. The construction of the *Tg737* expression construct (Tg737Bap) and transfection of BroF2 liver and 94D renal cells was described previously with Lipofectamine plus according to the manufacturer's protocol (Life Technologies, Gaithersburg, MD) (Richards *et al.*, 1997; Yoder *et al.*, 1997). Stable clonal cell lines were generated by drug selection with 400 $\mu$g $ml^{-1}$ G418. Immunolocalization studies performed on polarized MDCK cells were conducted using confluent cultures grown on Transwell filters for a minimum of 3 d to establish full epithelial polarization.

### *Maintenance of Mice and Histological Analysis*

The generation and genotyping of the $Tg737^{orpk}$ and $Tg737^{\Delta 2\text{-}3\beta Gal}$ mutant mouse lines has been described previously (Yoder *et al.*, 1997; Murcia *et al.* 2000). For histological examination of cilia, brains were isolated from age-matched mutant and wild-type adult mice, cut into small coronal blocks, fixed in 4% formaldehyde, embedded in paraffin, and cut into 5-$\mu$m sections following standard procedures. Tissue sections were counterstained with hematoxylin and eosin or nuclear fast red. The same regions in both the mutants and wild-type brains were photographed using the Nikon Coolpix 900 digital camera and differential interference contrast microscopy. All mice were maintained at the University of Alabama School of Medicine according to National Institutes of Health guidelines.

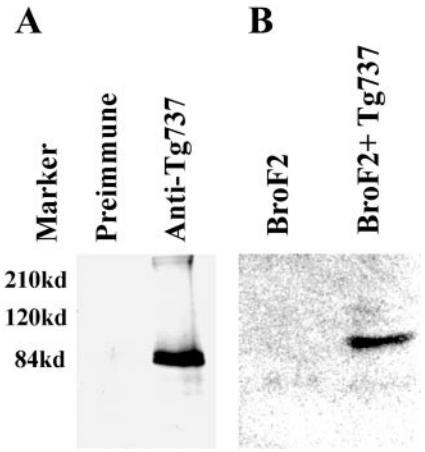


**Figure 1.** Characterization of the anti-Polaris antisera. (A) Specificity of the anti-Polaris antisera was evaluated by immunoprecipitation of in vitro translated Polaris. The immune serum immunoprecipitated a protein product of the expected size, whereas no product was seen using the corresponding preimmune serum. (B) Specificity of the antibodies was tested on Western blots by using mutant BroF2 liver cells transfected with the *Tg737* expression cassette. A 95-kDa product corresponding to full-length Polaris was seen only in the transfected cells (BroF2 + Tg737) but not in nontransfected cells (BroF2).

## RESULTS

### *Anti-Polaris Antibody Characterization*

Polyclonal anti-Polaris antibodies were generated in four rabbits by using a 21 amino acid synthetic peptide corresponding to the N terminus of mouse Polaris. Sera from three of the rabbits (GN593, GN1439, and GN1440) tested positive for the peptide by enzyme-linked immunosorbent assay and were affinity purified. Several experiments were conducted to evaluate the antisera. First, crude and preimmune sera were used to immunoprecipitate radiolabeled in vitro translated Polaris (Figure 1A). Anti-Polaris but not the preimmune serum was capable of immunoprecipitating a protein of the expected molecular weight (~95 kDa). Identical results were obtained using the affinity-purified antisera from all three rabbits. To further evaluate the specificity, Western blot analysis was conducted on *orpk* mutant liver cells and collecting duct cells (BroF2 and 94D, respectively) transfected with the *Tg737-β-actin* promoter construct. The *Tg737-β-actin* construct encodes a functional Polaris protein as demonstrated in transgenic rescue experiments (Moyer *et al.*, 1994; Yoder *et al.*, 1995). With the affinity purified anti-Polaris antisera, a protein of ~95 kDa was detected only in lysates from the rescued cells (Figures 1B, and 2, A and B). The level of expression in the 94D cells is similar to endogenous levels in the kidney and thus the Western result is not simply an artifact of overexpression of the cDNA. Furthermore, Western blot analysis of extracts from the $Tg737^{orpk}$ mutant and wild-type kidney, lung, brain, and testis all demonstrate the loss of this 95-kDa protein, which is in agreement with the disruption of *Tg737* in *orpk* mutant mice (Figure 2A, shown for kidney). Although these data indicate the antisera recognizes the protein encoded by *Tg737* cDNA, in all samples analyzed there was an additional protein detected at varying levels with a molecular weight of ~75 kDa. We predict that this smaller protein is an isoform of Polaris that arises from alternative splicing. To evaluate this possibility, we conducted Western blot analysis on protein extracts isolated form $Tg737^{\Delta 2\text{-}3\beta Gal}$ embryos at prenatal day 8.0. As seen for the kidney, two prominent proteins with molecular weight of 95 and 75 kDa were detected in wild-type embryo extracts. In contrast, both proteins were absent in extracts from the $Tg737^{\Delta 2\text{-}3\beta Gal}$ null allele (Figure 2D). Thus, we conclude that the 75-kDa protein is a Polaris isoform and that the antibody is specific for the *Tg737* protein product. The antibody specificity is further supported by the direct correlation between the spatial localization of the endogenous *Tg737* promoter-driven *β*-galactosidase activity and immunolocalization of the Polaris protein as demonstrated in the following section.

### *Polaris Expression in Mutant and Wild-Type Mice*

To determine the distribution of Polaris expression in the mouse, Western blot analysis was performed on lysates generated from wild-type mouse tissues. Similar to the Northern results, tissues expressing the highest levels of Polaris are the testis, brain, kidney, and lung (our unpublished results). In contrast, in the heart, spleen, and liver Polaris was nearly undetectable. As mentioned above, two proteins are detected by the antisera (Figure 2A, shown for kidney). The larger protein was ~95 kDa, in close correlation with the size predicted from the *Tg737* cDNA sequence and identical in size to the protein detected in transfected cell lines. The smaller protein is likely to be a Polaris isoform because its expression is not detected in extracts isolated from the null $Tg737^{\Delta 2\text{-}3\beta Gal}$ mutant embryos (Figure 2D). This conclusion is further supported by the expression of the 75-kDa product that paralleled that of the 95-kDa protein in all wild-type tissues analyzed. In other words, if a tissue expressed the 95-kDa protein the smaller peptide was also expressed. Conversely, if a tissue did not express the 95-kDa protein, then the 75-kDa protein was not detectable either. These data suggest that the 75-kDa protein is regulated in a similar manner as the 95-kDa protein and that it is a Polaris isoform. We predict from the multiple *Tg737* transcripts seen on Northern blots that this smaller protein is generated by alternative splicing of the mRNA (Figure 2, D and E); Moyer *et al.*, 1994; Murcia *et al.*, 2000).

In agreement with *Tg737*'s role in the mutant pathology, Western blot analysis of lysates from $Tg737^{orpk}$ mutant tissues failed to detect the 95-kDa product; however, as mentioned above, the 75-kDa protein was still present (Figure 2A). In most experiments, the level of expression of the 75-kDa protein appeared to increase in mutant extracts relative to the wild-type control. This phenomenon could be reversed upon reexpression of the *Tg737* cDNA in $Tg737^{orpk}$ mutant collecting duct cells or mutant liver cells (Figure 2, B and C). This result suggests that expression of the 75-kDa protein may be under autoregulatory control. The continued expression of a Polaris protein in mutant tissues is not a surprising result. As seen in Northern blots, several transcripts that are detected in wild-type tissues persist in $Tg737^{orpk}$ mutant mice (Figure 2E). This is particularly relevant in the testis where as many as five transcripts have been detected ranging in size from 2.8 to 6.0 kb; whether all of these transcripts encode a Polaris isoform remains to be

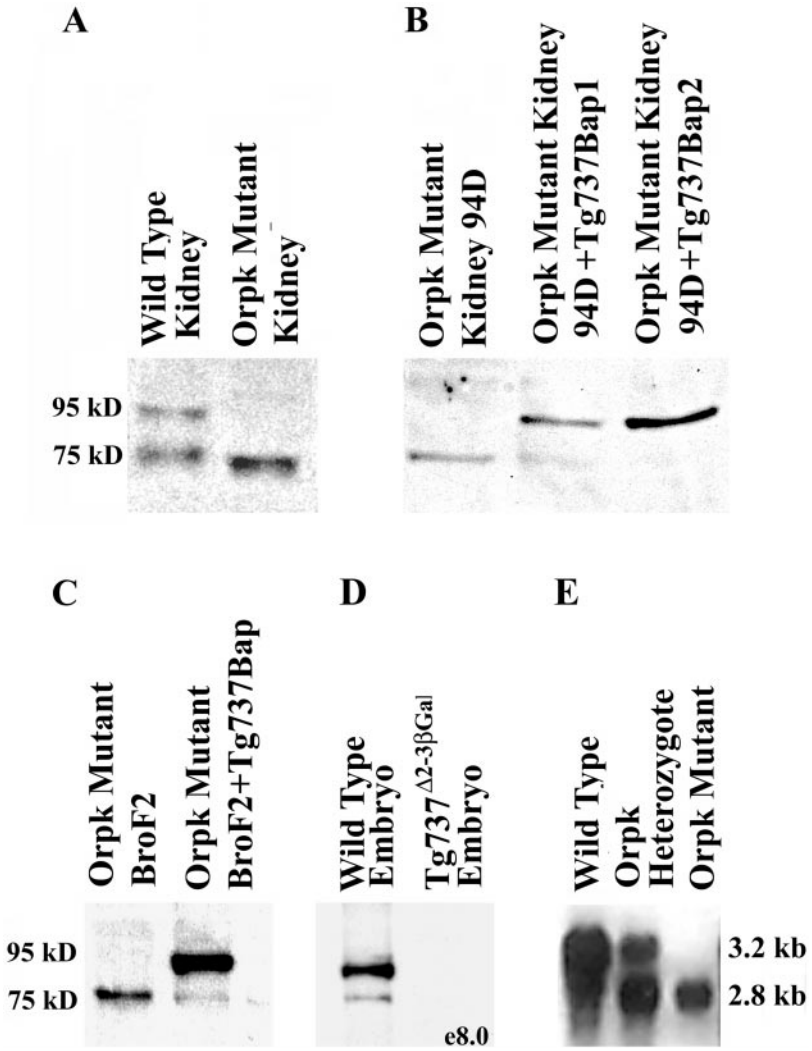


**Figure 2.** Polaris and Tg737 expression in mutant and wild-type samples. (A) Analysis of Polaris expression in mutant kidney extracts reveals that expression of the 95-kDa protein is abolished; however, the levels of the 75-kDa isoform increased. The small shift in the size of the 75-kDa isoform in the mutant sample is due to slightly aberrant running during electrophoresis. (B) Level of expression of the smaller protein isoform was inversely correlated with the level of expression of the 95-kDa product in 94D *Tg737*$^{orpk}$ mutant collecting duct cell line. (C) As seen in the collecting duct cell line, expression of the 95-kDa Polaris peptide reduced the level of the putative 75-kDa isoform. (D) Western blot analysis revealed that expression of both the ~95 kDa and ~75 kDa proteins are abolished in e8.0 *Tg737*$^{\Delta 2\text{-}3\beta\text{-Gal}}$ mutant embryos. (E) Northern analysis was conducted on Poly(A$^+$) selected RNA from wild-type, *Tg737*$^{orpk}$ heterozygous, and *Tg737*$^{orpk}$ homozygous mutant testis. *Tg737* expression was detected as two prominent transcripts corresponding to 2.8 and 3.2 kb in both wild-type and heterozygous samples. In mutants, the 3.2-kb transcript is lost, whereas expression of the smaller transcript persists. Similar results are obtained in other tissues except that higher molecular weight transcripts are also present.

determined. From these data we predict that the continued expression of the lower molecular weight protein in mutants is due to the hypomorphic nature of the *Tg737*$^{orpk}$ allele. This is supported by the dramatic change in phenotype between homozygous *Tg737*$^{orpk}$ and *Tg737*$^{\Delta 2\text{-}3\beta Gal}$ mice and the loss of the 75-kDa protein in extracts from null mutants (Moyer *et al.*, 1994; Murcia *et al.*, 2000).

### *Spatial Expression of* Tg737 *and Localization of Polaris*

Northern blot analyses indicate that *Tg737* is expressed ubiquitously in all tissues analyzed to date. To determine which cells express *Tg737* and where Polaris might function in these cells, we used the β-galactosidase reporter gene incorporated into the *Tg737*$^{\Delta 2-3\beta Gal}$ targeting construct described previously and the affinity-purified anti-Polaris antisera from three different rabbits to identify *Tg737*-expressing cells in vivo. The *Tg737*$^{\Delta 2\text{-}3\beta Gal}$ construct was generated such that upon homologous recombination, the endogenous *Tg737* promoter would direct expression of β-galactosidase (Murcia *et al.*, 2000).

### *Tg737 and Polaris in Ciliated Lung Epithelium*

In the lung, *Tg737* expression was prominently detected in the distal bronchioles and in the trachea; however, not all cells lining the bronchiole were β-galactosidase positive (Figure 3, A and B). Immunofluorescence analysis with the anti-Polaris antibody produced a signal in the same areas of the lung as the β-galactosidase staining. This correlation of the β-galactosidase staining, both at the level of expression and spatial distribution, with the immunolocalization data strongly support that the antibodies used in this study are recognizing Polaris, regardless of whether its the 75- or 95-kDa protein (Figure 3C). Subcellularly, Polaris concentrated below the apical surface and in projections extending into the bronchiole lumen (Figure 3C, inset). To determine whether the projections were cilia, we probed sections with anti-β-tubulin IV, a core constituent of the cilia axoneme

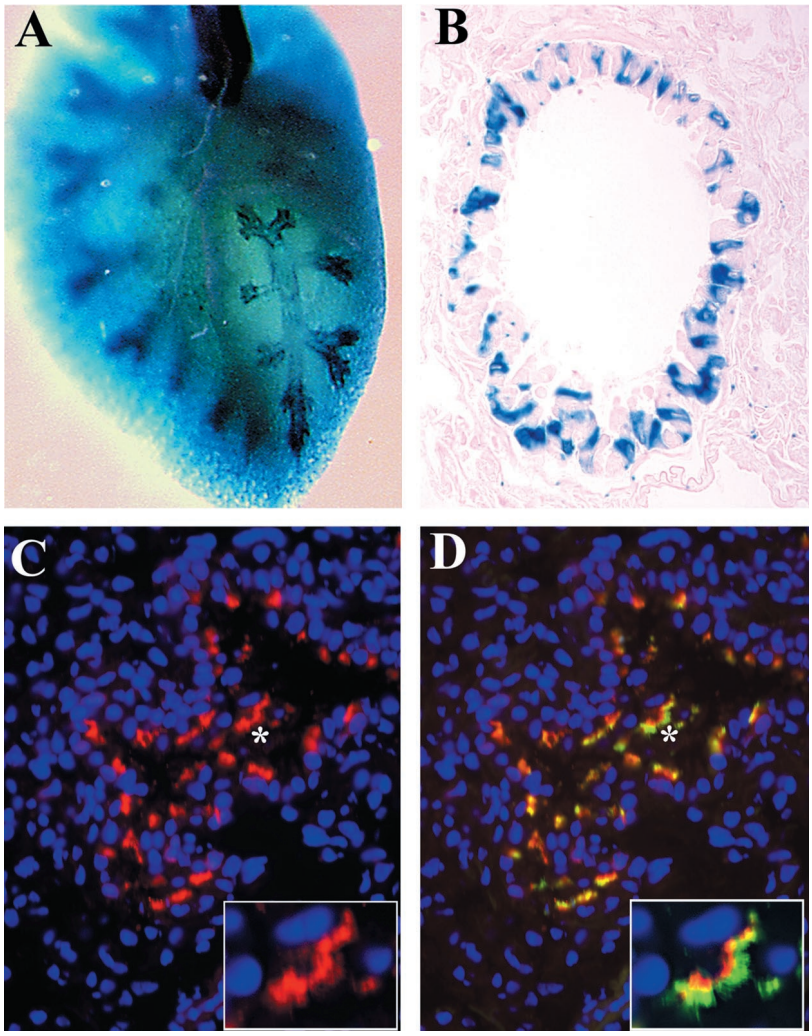


**Figure 3.** Tg*737* and Polaris expression is associated with ciliated epithelia of the lung. (A) In whole mounts, *Tg737* expression as revealed by β-galactosidase activity was prominently detected in the distal bronchioles and in the trachea. (B) In sections, not all cells lining the bronchioles were found to express *Tg737*. (C and D) Similar results were obtained when Polaris localization was determined using immunofluorescence where both expressing and nonexpressing cells were evident. Polaris (red) expression was only seen in cells that also express β-tubulin (green). Closer examination of the regions in C and D marked by the asterisks indicate that Polaris is most concentrated in a band in the apical cytoplasm of the epithelium (C) and in small projections that are also positive for β-tubulin (D).

(Renthal *et al.*, 1993). All Polaris-positive cells also expressed high levels of β-tubulin (Figure 3D, inset). Those cells in the bronchioles and trachea that failed to express Polaris were not ciliated as determined by the lack of β-tubulin expression. Thus, in the lung Polaris was specific to the basal bodies and cilary axoneme of ciliated epithelium.

### *Polaris during Sperm Maturation and in the Testis*

By Northern and Western blot analyses, high levels of *Tg737* and Polaris expression were detected in the male and female reproductive tracts (oviduct and testis/epididymis; our unpublished results). Expression of *Tg737* in the testis was complex, where more β-galactosidase–positive cells were present in the periphery of the seminiferous tubules than near the tubule lumen (Figure 4A). Because spermatogenesis occurs in a wavelike manner with the immature spermatogonia located at the periphery and more differentiated late spermatids occupying the inner portion of the tubule, it is likely that the β-galactosidase–expressing cells are spermatogonium and primary spermatocytes, a result supported by the morphology of the cells (Leblond and Clermont, 1952). In contrast to the β-galactosidase staining, higher levels of Polaris are seen in the mature flagellated sperm than in the immature cells (Figure 4B). Polaris localization in the sperm was concentrated in the basal body region from which the flagella emerged (Figure 4B). Similar to the cilia in the lung, low levels of Polaris could be detected in the flagella axoneme. There was significant colocalization between Polaris and β-tubulin; however, the latter invariantly extended further toward the acrosome (Figure 4, B–D). The discrepancy between β-galactosidase activity and immunofluorescence in the testis likely reflects the transcriptional inhibition that occurs during sperm differentiation and reduced Polaris turnover in the mature sperm.

To determine whether *Tg737* expression was associated with ciliated epithelium outside the lung, we analyzed expression in the efferent duct, which contain extensive motile cilia (Figure 5, A and B). Both β-galactosidase activity and Polaris expression were specific to the epithelium and were significantly elevated relative to that seen in the seminiferous tubules. Cells expressing Polaris invariantly expressed high levels of β-tubulin. As

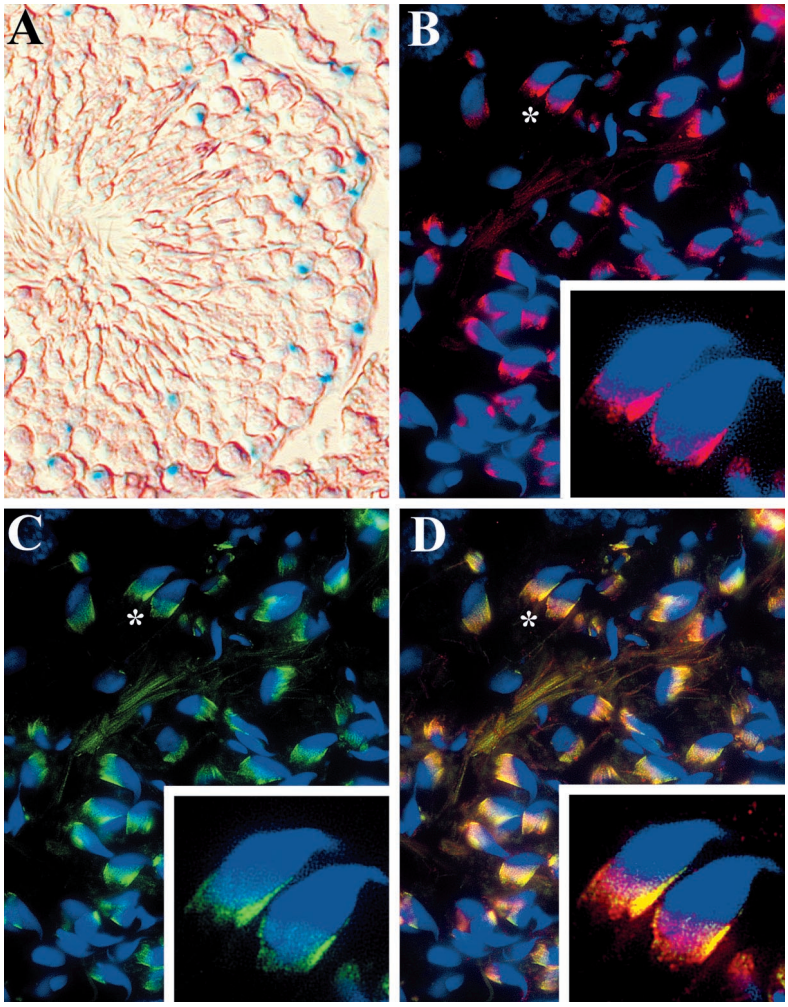


**Figure 4.** Tg737 and Polaris expression and localization during sperm maturation. (A) Polaris expression was analyzed using the β-galactosidase reporter in the seminiferous tubules of the adult testis. *Tg737* expression was detected in cells at the periphery and not in cells located near the tubule lumen. (B) In contrast to the β-galactosidase results, no Polaris expression could be detected in the cells of the periphery of the seminiferous tubules, but high levels were present in mature sperm within the seminiferous tubules. Polaris was concentrated on the same side of the hook in the mouse sperm in the region of the centriole (inset). Polaris could also be detected in the flagella axoneme. (C and D) A nearly identical staining pattern was seen for β-tubulin in the mature sperm; however, β-tubulin invariantly extended further up the sperm head (inset).

seen in the lung, Polaris was localized to the cilia axoneme and basal bodies (Figure 5, C and D).

### *Tg737 in Renal Tubules and Polaris Localization in MDCK Cells*

The *Tg737*$^{orpk}$ mutants develop renal cysts that arise in most segments of the nephron, but the collecting ducts appear to be the most severely effected (Yoder *et al.*, 1995, 1996). Low levels of β-galactosidase activity were detected in most segments of the nephron in the cortex and the medulla (Figure 6, A and B). The reason for the punctate nature of the β-galactosidase staining in comparison to the diffuse cytoplasmic localization as seen in the lung, ependymal cells, or efferent duct is currently unknown. Due to this punctate pattern, many of the cells appeared not to express *Tg737* in individual sections. However, upon serial section analysis, we determined that this is not the case. Rather, *Tg737* as measured by β-galactosidase activity is present in almost all cells along the nephron and in many cells of the glomerulus. Thus, the failure to see β-galactosidase activity in some cells in the section shown is due to level at which the section was taken relative to the spot of β-galactosidase activity.

Interestingly with regard to our proposed role for Polaris, cilia have been detected on cells in the parietal layer of Bowman's capsule, as well as on epithelium of the proximal and distal tubules, and collecting duct (Bulger *et al.*, 1974; Webber and Lee, 1975). To evaluate whether Polaris is associated with the renal cilia, we attempted to colocalize Polaris and β-tubulin by immunofluorescence in vivo in the kidney. Unfortunately, we were unable to conduct this analysis due to autofluorescence in renal sections and the lower levels of Polaris associated with cells that posses only a monocilium. To circumvent this difficulty, we used polarized MDCK cells grown on Transwell filters that form a single cilium when cultured under these conditions. In support of the difficulties with the in vivo analysis in the kidney, Polaris was detected as a single very faint dot in the center of each cell as revealed by costaining with an antibody against the tight junction protein ZO-1 (Figure 6C). At higher magnification, staining for β-tubulin shows that a single cilium extends from this Polaris-positive region (Figure 6D). Polaris was also evident in a punctate pattern within the axoneme shaft reminiscent of intraflagellar transport rafts (Figure 6D, inset) (Cole *et al.*, 1998).

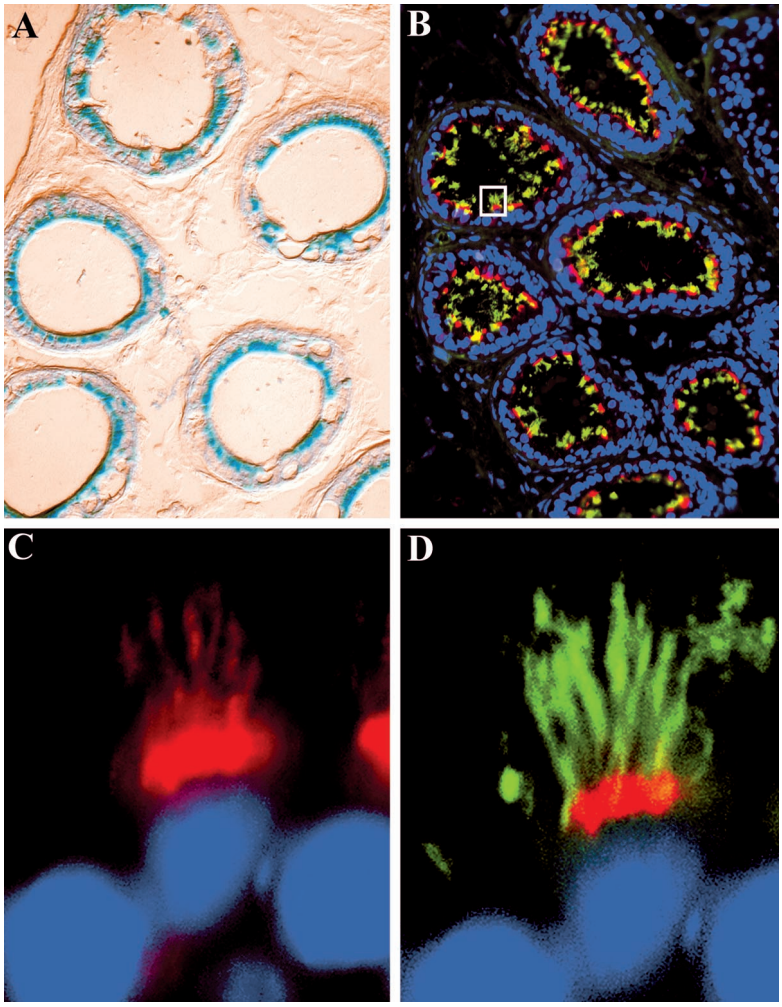


**Figure 5.** Tg737 and Polaris expression is associated with ciliated epithelium in the efferent duct. (A) *Tg737* expression (blue) in the efferent duct appears to be restricted to the epithelium with no activity detected in the interstitial cells. (B) Similar to the results for the β-galactosidase assay, Polaris (red) was detected in the epithelium. These epithelial cells contain multiple cilia, as revealed by costaining with β-tubulin (green). (C and D) Higher magnification of the boxed region in B shows that Polaris is concentrated at the apical surface of the cells and extends into the cilia axonemes.

### *Polaris Is Associated with Ciliated Cells in the Brain*

In the $Tg737^{\Delta 2\text{-}3\beta Gal}$ heterozygotes brain, the highest levels of β-galactosidase activity are seen in the ependymal cells lining the ventricles (Figure 7D). These epithelia have extensive cilia on their apical surface that extend into the ventricular lumen where they assist in movement of cerebral spinal fluid (Satir and Sleigh, 1990). As seen in the lung and efferent duct, dual staining with anti-Polaris and anti-β-tubulin confirmed that Polaris expression is associated with these ciliated epithelia (Figure 7, A–C). Low levels of *Tg737* expression were also seen in the choroid plexus by using the β-galactosidase reporter (Figure 7A). Similar to the results in the renal cell lines, Polaris expression was detected as a faint dot in the choroid plexus epithelium near the nucleus from which cilia project as revealed by β-tubulin staining (Figure 7, B and C, inset). Again, the tight relationship between the β-galactosidase expression and immunolocalization results suggests that our antisera are recognizing Polaris.

In addition to the high levels of Polaris in the ependymal cells, *Tg737* expression was evident in other regions of the adult brain such as cells within the hippocampus and the dentate gyrus and in the Purkinje and granular cell layer in the cerebellum (Figure 7, E and F). Attempts to localize Polaris in these cells by immunofluorescence were unsuccessful. Although there were no overt cilia evident on these cells as determined by β-tubulin localization, reports have described the presence of a single cilium on hippocampal and Purkinje cells by immunoelectron microscopy (Del Cerro and Snider, 1969). Thus, it is likely that Polaris is associated with the basal bodies in these cells as seen in MDCK cells and choroid plexus as described previously.

### *Hydrocephalus and Ciliary Defects in* $Tg737^{orpk}$ *Mutants*

*Tg737* expression data, along with the localization of the protein at the base of cilia, suggests that Polaris functions in a ciliogenic pathway. To determine whether the pathologies in $Tg737^{orpk}$ mice are related to ciliary defects, we analyzed paraffin-embedded sections of wild-type and mutant mice by differential interference contrast microscopy. In the kidney, we were unable to identify the monocilia on cells in the collecting duct in either wild-type or mutant samples. There-

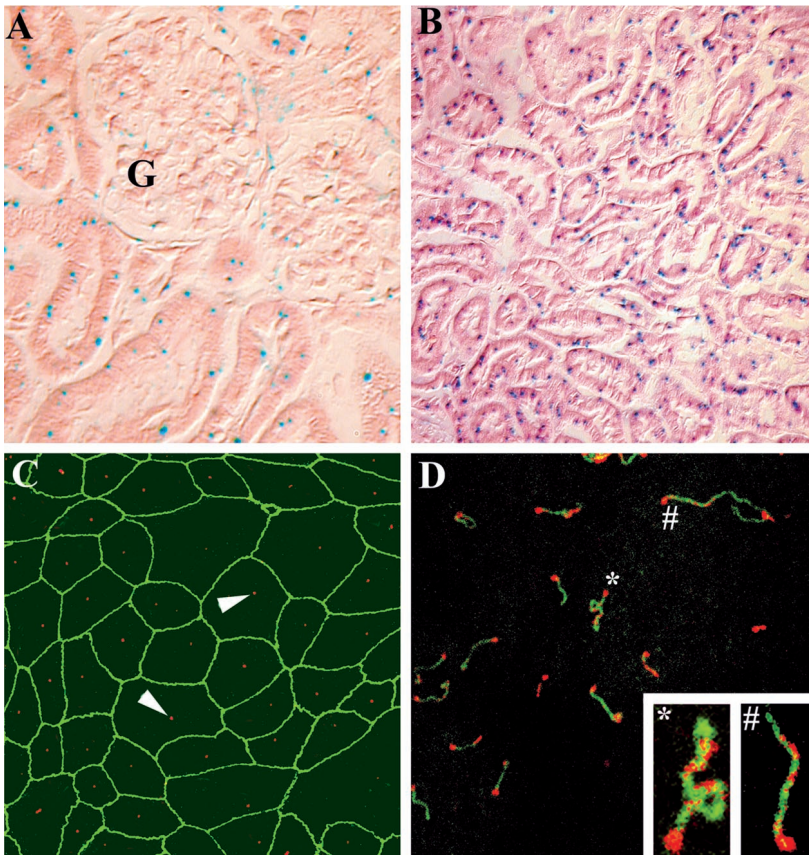


**Figure 6.** Tg737 expression in the kidney and localization of Polaris to basal bodies in MDCK cells. (A and B) Expression analysis with the β-galactosidase reporter gene (blue) indicates that most cells in the nephron express *Tg737*. *Tg737* is expressed in the glomerulus (G) and in almost all cells of the nephron in sections taken from either the cortex (A) or the medulla (B). (C) In polarized MDCK cells, a faint domain of Polaris (red, arrowhead) was detected near the apical surface in the cell. ZO-1, a protein localized to the tight junctions, is shown in green. (D) Immunolocalization of Polaris and β-tubulin indicate that Polaris is at the base of the cilia. At higher magnification, Polaris is seen in the axoneme of the cilia (insets) in a punctate pattern.

fore, we chose to analyze the ependymal cells lining the ventricles in the brain. This region was chosen because *Tg737* expression was highest in these cells and because the ependymal cells are extensively ciliated. In coronal sections of wild-type mouse brain, numerous cilia were observed on the ependymal cells extending into the ventricular lumen (Figure 8B). In contrast, there are significantly fewer cilia lining the ventricular lumen of the $Tg737^{orpk}$ brain (Figure 8A). The sparse cilia that were present were significantly smaller than cilia in wild-type mice, and appeared disorganized. It was also discovered during the analysis that $Tg737^{orpk}$ mutants exhibit hydrocephalus, a phenotype often associated with left-right patterning abnormalities and ciliary defects on the ependymal cells (Shimizu and Koto, 1992; Nakamura and Sato, 1993; Chen *et al.*, 1998). In all adult $Tg737^{orpk}$ mutants analyzed, the ventricles were expanded relative to controls (Figure 8, C and D). At this time, we are uncertain whether the expansion of the ventricles leads to the loss of cilia on the ependymal cells or whether the $Tg737^{orpk}$ ciliary defect contributes directly to this pathology.

## DISCUSSION

Partial loss of *Tg737* function in $Tg737^{orpk}$ mutant mice leads to severe pathology in the kidney, brain, liver, pancreas, and skeleton, whereas complete loss of *Tg737* in $Tg737^{\Delta 2\text{-}3\beta Gal}$ mutants results in mid-gestational lethality and random left-right axis determination (Moyer *et al.*, 1994; Murcia *et al.*, 2000). We used the β-galactosidase reporter gene incorporated into the $Tg737^{\Delta 2\text{-}3\beta Gal}$ allele and anti-Polaris antisera to determine whether *Tg737* expression is associated with a specific cell type or whether Polaris is concentrated in any cellular domain. With either assay, *Tg737* expression was detected mainly in sperm and ciliated epithelium, with the level of β-galactosidase activity and Polaris expression paralleling the number of cilia found on a cell. In both multi- and monociliated epithelium and in sperm, Polaris was localized to the basal bodies and in the axoneme. Although detection of two proteins on Western blots complicates the interpretation of the immunofluorescence data, the loss of both proteins in *Tg737* null mutants along with the correlation between the β-galactosidase activity and immunofluorescence localization and the ciliary defects associated with *Tg737* mutations, we predict a ciliogenic role for Polaris.

Polaris staining in the axoneme and basal bodies is similar to that reported for proteins involved in IFT (Kozminski *et al.*, 1995; Cole *et al.*, 1998). These proteins accumulate at the base of cilia in the region of basal bodies where they form large rafts. The IFT rafts are transported along the axoneme by the action of the heterotrimeric kinesin-II complex (*Kif3A*, *Kif3B*, and *Kap*) and dyneins. Interesting, disruption of either of the kinesins in mice results in loss of cilia and LR patterning defects that are remarkably similar to $Tg737^{\Delta 2\text{-}3\beta Gal}$ mutants (Nonaka *et al.*, 1998; Marszalek *et al.*, 1999; Takeda *et al.*, 1999). Thus, these data along with the localization of

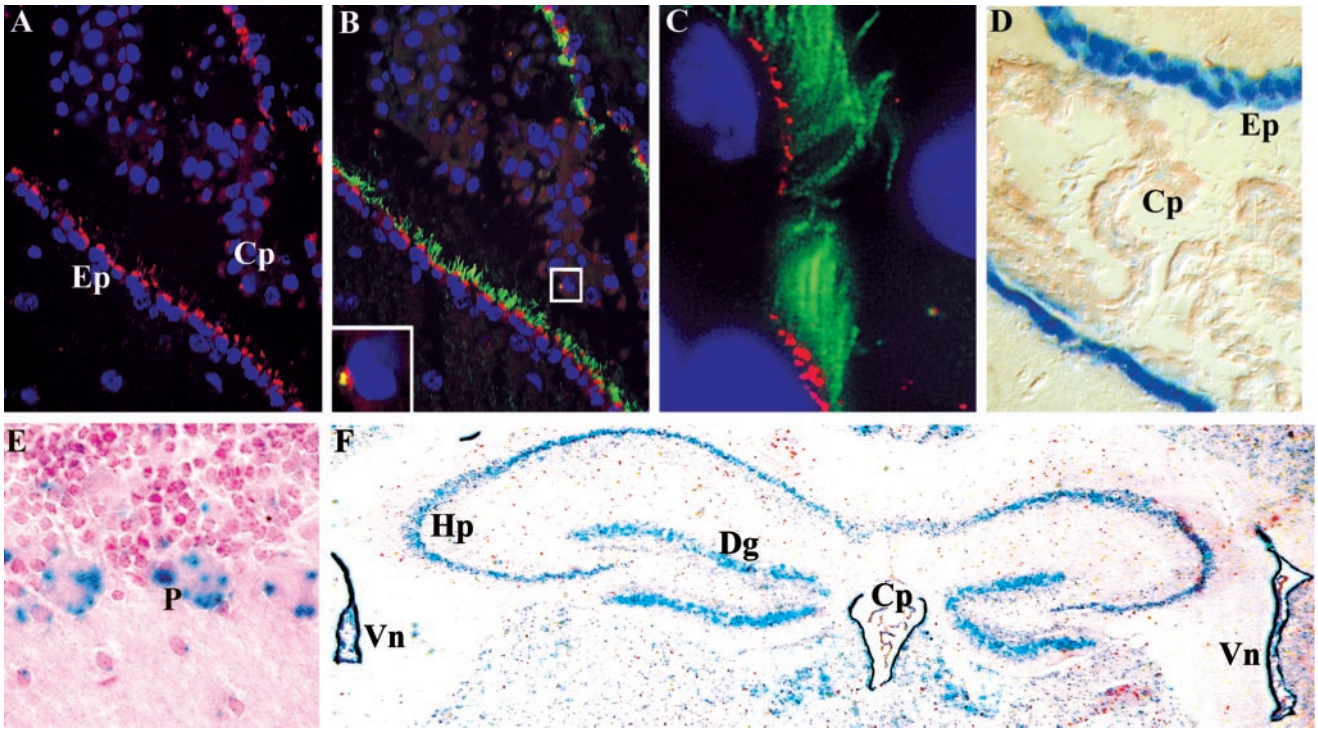


**Figure 7.** Tg737 and Polaris expression and localization in ciliated cells in the brain. (A) High levels of Polaris (red) expression were detected near the apical surface of ependymal cells lining the ventricles of the brain with significantly lower expression in cells of the choroid plexus. (B and C) Ependymal cells are extensively ciliated as revealed by β-tubulin (green) expression. Polaris was found at the base of each cilium. Identical localization was seen in the choroid plexus (B, inset) where short cilia were detected emerging off a small domain of Polaris. (D) With the β-galactosidase reporter gene, high levels of *Tg737* expression were seen in the ependymal cells with lower expression in the choroid plexus. (E and F) In addition to the epithelial cells lining the ventricles (Vn) and in the choroid plexus (Cp), *Tg737* expression was seen in the Purkinje (P) cells in the cerebellum (E) and in the cells of the hippocampus (Hp) and the dentate gyrus (Dg) (F).

Polaris to the basal bodies and cilia axoneme suggest that Polaris may be involved in a similar process during cilia formation as the kinesins. Polaris, with its 10 tetratricopeptide repeat motifs may serve as the scaffold upon which IFT proteins assemble. Such a function for a TPR-containing protein would not be too unexpected because TPR-containing proteins have been shown to mediate large protein complex formation (Moyer *et al.*, 1994; Blatch and Lassle, 1999). Alternatively, Polaris may simply be cargo that becomes incorporated into the cilium where it plays a yet-to-be-identified function. Identification of proteins that interact with Polaris, coimmunolocalization studies at the level of

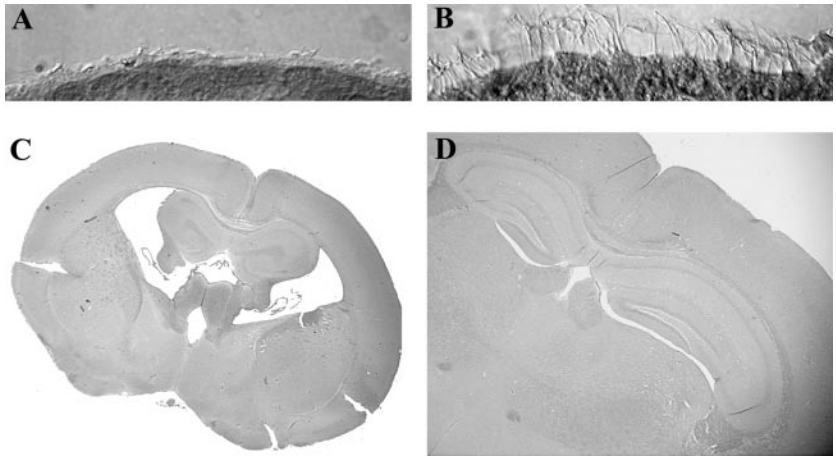


**Figure 8.** Hydrocephalus in *Tg737*$^{orpk}$ mutants and ciliary defects on the ependymal cells. (A) Very few cilia were present on the ependymal cells lining the ventricles of all the *Tg737*$^{orpk}$ mutant mice analyzed. (B) In contrast, abundant cilia are present on these cells in the wild-type mice. (C) Hydrocephalus was evident in all mutant mice analyzed. (D) There was no ventricular expansion in any of the wild-type controls.

electron microscopy, and detailed analysis of the Polaris homologs in simpler organisms should help elucidate these possibilities.

During the course of this study, we noted that *Tg737*$^{orpk}$ mutants develop hydrocephalus. Hydrocephalus results from increased intercranial pressure due to improper homeostasis or movement of the cerebral spinal fluid, and is often associated with ciliary abnormalities on ependymal cells lining the ventricles (Shimizu and Koto, 1992; Nakamura and Sato, 1993; Chen *et al.*, 1998). Because these cells also express high levels of *Tg737*, we evaluated whether they have ciliary defects in *Tg737*$^{orpk}$ mutants. In all mutants analyzed, the number of cilia was dramatically reduced and those present were shorter and disorganized. Although the protein localization described here and the phenotype described previously in *Tg737*$^{\Delta 2\text{-}3\beta Gal}$ mutants suggest a role for Polaris in ciliogenesis, we cannot exclude the possibility that the loss of cilia is a consequence of increased intercrainal pressure rather than a contributing factor (Bannister and Chapman, 1980). Correlating the temporal development of the hydrocephalus phenotype with the affects on cilia will distinguish between these possibilities.

An intriguing observation is that there appears to be a connection between left-right patterning and kidney defects. This is seen in mice lacking normal *Tg737* function and the *inv* mutant, both of which develop cystic lesions in the kidney. Similar pathology has been reported in humans, leading to the proposal that situs inversus associated with cystic kidney disease constitutes a pathological syndrome (Moyer *et al.*, 1994; Mochizuki *et al.*, 1998; Balci *et al.*, 2000; Murcia *et al.*, 2000). Like the node, the epithelial cells lining much of the nephron contain a single cilium. In both cases, the cilia exhibit a 9 + 0 microtubule arrangement characteristic of primary cilium (Nonaka *et al.*, 1998). The cilia on the node are one of the few examples of primary cilia known to be motile. Whether renal cilia perform a similar function with regard to fluid movement or act as organelles responsible for sensing local environment remains to be explored. Elucidating the biological role of genes such as *Tg737* and *inv* that affect both renal and node cilia should provide important clues to the function of these specialized structures and help reveal how their loss leads to the mutant phenotypes.

Several mutations that affect left-right patterning have now been characterized in the mouse (Nonaka *et al.*, 1998; Marszalek *et al.*, 1999; Okada *et al.*, 1999; Supp *et al.*, 1999; Takeda *et al.*, 1999). In most cases, the alterations in axis determination are associated with ciliary defects or nodal flow. Although the loss of cilia is suggestive that these proteins act in a ciliogenic pathway, it is equally plausible that cilia are lost due to an unrelated event. This could occur simply by altered cell polarity involving protein transport or lack of normal differentiation of cells in the node. This is particularly relevant to the *Tg737*$^{orpk}$ mutant because one of the hallmarks of the pathology is continued proliferation of immature epithelium. Although we have not analyzed Polaris in node cells, its localization to cilia in cells of other tissues would suggest that the pathology in *Tg737*$^{orpk}$ mutants and the left-right defect in *Tg737*$^{\Delta 2\text{-}3\beta Gal}$ mice are not caused by a general loss of cellular differentiation or cell cycle control, but rather by the defects in a ciliogenic pathway.

The association of *Tg737* and ciliogenesis is further supported by the similarities in the pattern of *Tg737* expression and that of *Hfh4*, a forkhead transcription factor involved in differentiation of epithelium possessing motile cilia (Chen *et al.*, 1998; Blatt *et al.*, 1999). In the lung, brain, testis, and embryonic node, the expression of *Tg737* is identical to that of *Hfh4*. In contrast to *Hfh4*, *Tg737* expression is detected in cells that have immotile primary cilia, such as Purkinje and hippocampal cells and renal epithelium (Del Cerro and Snider, 1969; Bulger *et al.*, 1974; Webber and Lee, 1975). Interestingly, *Hfh4* mutants also develop hydrocephalus with alterations in cilia on the ependymal cells and random left-right axis patterning (Chen *et al.*, 1998). However, although node cilia are lost in the *Tg737* knockout mutant, the node cilia in *Hfh4* mutants appear normal (Brody *et al.*, 2000). It remains to be determined whether the motility and nodal flow are affected in these mutants, as they are in *iv* mice. As suggested previously, these selective affects on motile and immotile cilia imply that they may be formed through slightly different mechanisms (Brody *et al.*, 2000). Further analysis of the relationship between *Tg737*, *Hfh4, lrd*, *inv, Kif3A*, *Kif3B*, and other factors involved in ciliogenesis will be required to elucidate this complex process and its role in normal patterning of the mammalian embryo.

## ACKNOWLEDGMENTS

We gratefully acknowledge Drs. William Richards and Ed Michaud for their critical reading of the manuscript. We also thank Albert Tousson and Shawn Williams of the University of Alabama at Birmingham High Resolution Imaging Facility for their assistance in image generation. The research described in this manuscript was supported by a grant to B.K.Y. from National Institute of Diabetes and Digestive and Kidney Diseases (1RO1 DK-55007-01). Additional support was provided by the Polycystic Kidney Research Foundation (Grant 99028) and the Medical Research Service of the Department of Veterans Affairs to D.F.B. D.F.B. is a recipient of a Veterans Affairs Career Development Award.

## REFERENCES

Afzelius, B. (1976). A human syndrome caused by immotile cilia. Science *193*, 317–319.

Balci, S., Boostanoglu, S., Altinok, G., and Ozaltin, F. (2000). Three sibs diagnosed prenatally with situs inversus totalis, renal and pacreateic dysplasia and cysts. Am. J. Med. Genet. *90*, 185–187.

Balkovetz, D.F., Pollack, A.L., and Mostov, K.E. (1997). Hepatocyte growth factor alters the polarity of Madin-Darby canine kidney cell monolayers. J. Biol. Chem. *272*, 3471–3477.

Bannister, C.M., and Chapman, S.A. (1980). Ventricular ependyma of normal and hydrocephalic subjects: a scanning electronmicroscopic study. Dev. Med. Child Neurol. *22*, 725–735.

Blatch, G.L., and Lassle, M. (1999). The tetratricopeptide repeat: a structural motif mediating protein-protein interactions. Bioessays *21*, 932–939.

Blatt, E.N., Yan, X.H., Wuerffel, M.K., Hamilos, D.L., and Brody, S.L. (1999). Forkhead transcription factor HFH-4 expression is temporally related to ciliogenesis. Am. J. Respir. Cell Mol. Biol. *21*, 168–176.

Brody, S.L., Yan, X.H., Wuerffel, M.K., Song, S.-K., and Shapiro, S.D. (2000). Ciliogenesis and left-right axis defects in forkhead factor Hfh-4-null mice. Am. J. Respir. Cell. Mol. Biol. *23*, 45–51.

Bulger, R.E., Siegel, F.L., and Pendergrass, R. (1974). Scanning and transmission electron microscopy of the rat kidney. Am. J. Anat. *139*, 483–501.

Chen, J., Knowles, H.J., Hebert, J.L., and Hackett, B.P. (1998). Mutation of the mouse hepatocyte nuclear factor/forkhead homologue 4 gene results in an absence of cilia and random left-right asymmetry. J. Clin. Invest. *102*, 1077–1082.

Cole, D.G., Diener, D.R., Himelblau, A.L., Beech, P.L., Fuster, J.C., and Rosenbaum, J.L. (1998). Chlamydomonas kinesin-II-dependent intraflagellar transport (IFT): IFT particles contain proteins required for ciliary assembly in *Caenorhabditis elegans* sensory neurons. J. Cell Biol. *141,* 993–1008.

Del Cerro, M.P., and Snider, R.S. (1969). The purkinje cell cilium. Anat. Rec. *165*, 127–140.

Handel, M., Schulz, S., Stanarius, A., Schreff, M., Erdtmann-Vourliotis, M., Schmidt, H., Wolf, G., and Hollt, V. (1999). Selective targeting of somatostatin receptor 3 to neuronal cilia. Neuroscience *89*, 909–926.

Kozminski, K.G., Beech, P.L., and Rosenbaum, J.L. (1995). The Chlamydomonas kinesin-like protein FLA10 is involved in motility associated with the flagellar membrane. J. Cell Biol. *131*, 1517–1527.

Kozminski, K.G., Johnson, K.A., Forscher, P., and Rosenbaum, J.L. (1993). A motility in the eukaryotic flagellum unrelated to flagellar beating. Proc. Natl. Acad. Sci. USA *90*, 5519–5523.

Leblond, C.P., and Clermont, Y. (1952). Definition of the stages of the cycle of the seminiferous epithelium in the rat. Ann. NY Acad. Sci. *55*, 548–573.

Marszalek, J.R., Ruiz-Lozano, P., Roberts, E., Chien, K.R., and Goldstein, L.S. (1999). Situs inversus and embryonic ciliary morphogenesis defects in mouse mutants lacking the KIF3A subunit of kinesin-II. Proc. Natl. Acad. Sci. USA *96*, 5043–5048.

Mochizuki, T., Saijoh, Y., Tsuchiya, K., Shirayoshi, Y., Takai, S., Taya, C., Yonekawa, H., Yamada, K., Nihei, H., Nakatsuji, N., Overbeek, P.A., Hamada, H., and Yokoyama, T. (1998). Cloning of inv, a gene that controls left/right asymmetry and kidney development. Nature *395*, 177–181.

Moyer, J.H., Lee-Tischler, M.J., Kwon, H.Y., Schrick, J.J., Avner, E.D., Sweeney, W.E., Godfrey, V.L., Cacheiro, N.L., Wilkinson, J.E., and Woychik, R.P. (1994). Candidate gene associated with a mutation causing recessive polycystic kidney disease in mice. Science *264*, 1329–1333.

Murcia, N.S., Richards, W.G., Yoder, B.K., Mucenski, M.L., Dunlap, J.R., and Woychik, R.P. (2000). The Oak Ridge Polycystic Kidney (orpk) disease gene is required for left-right axis determination. Development *127*, 2347–2355.

Nakamura, Y., and Sato, K.Y. (1993). Role of disturbance of ependyaml ciliary function in development of hydrocephalus in rats. Childs Nerv. Syst. *9*, 65–71.

Nonaka, S., Tanaka, Y., Okada, Y., Takeda, S., Harada, A., Kanai, Y., Kido, M., and Hirokawa, N. (1998). Randomization of left-right asymmetry due to loss of nodal cilia generating leftward flow of extraembryonic fluid in mice lacking KIF3B motor protein [published erratum appears in Cell (1999) *99*, 117]. Cell *95*, 829–837.

Okada, Y., Nonaka, S., Tanaka, Y., Saijoh, Y., Hamada, H., and Hirokawa, N. (1999). Abnormal nodal flow precedes situs inversus in iv and inv mice. Mol. Cell *4*, 459–468.

Renthal, R., Schneider, B.G., Miller, M.M., and Luduena, R.F. (1993). Beta IV is the major beta-tubulin isotype in bovine cilia. Cell Motil. Cytoskeleton *25*, 19–29.

Richards, W.G., Yoder, B.K., Isfort, R.J., Detilleux, P.G., Foster, C., Neilsen, N., Woychik, R.P., and Wilkinson, J.E. (1997). Isolation and characterization of liver epithelial cell lines from wild-type and mutant TgN737Rpw mice. Am. J. Pathol. *150*, 1189–1197.

Sambrook, J., Fritsch, E.F., and Maniatis, T. (1989). Molecular Cloning: A Laboratory Manual, Cold Spring Harbor, NY: Cold Spring Harbor Laboratory Press.

Satir P.T., and Sleigh M.A. (1990). The physiology of cilia and mucociliary interactions. Annu. Rev. Physiol. *52*, 137–155.

Shimizu, A., and Koto, M. (1992). Ultrastructure and movement of the ependymal and tracheal cilia in congenitally hydrocephalic Wic-Hyd rats. Childs Nerv. Syst. *8*, 25–32.

Supp, D.M., Brueckner, M., Kuehn, M.R., Witte, D.P., Lowe, L.A., McGrath, J., Corrales, J., and Potter, S.S. (1999). Targeted deletion of the ATP binding domain of left-right dynein confirms its role in specifying development of left-right asymmetries. Development *126*, 5495–504.

Supp, D.M., Witte, D.P., Potter, S.S., and Brueckner, M. (1997). Mutation of an axonemal dynein affects left-right asymmetry in inversus viscerum mice. Nature *389*, 963–966.

Takeda, S., Yonekawa, Y., Tanaka, Y., Okada, Y., Nonaka, S., and Hirokawa, N. (1999). Left-right asymmetry and kinesin superfamily protein KIF3A: new insights in determination of laterality and mesoderm induction by kif3A−/− mice analysis. J. Cell Biol. *145*, 825–836.

Wagner, M.K., and Yost, H.J. (2000). Left-right development: the roles of nodal cilia. Curr. Biol. *10*, R149–R151.

Webber, W.A., and Lee, J. (1975). Fine structure of mammalian renal cilia. Anat. Rec. *182*, 339–343.

Wheatley, D.N., Wang, A.M., and Strugnell, G.E. (1996). Expression of primary cilia in mammalian cells. Cell Biol. Int. *20*, 73–81.

Yoder, B.K., Richards, W.G., Sommardahl, C., Sweeney, W.E., Michaud, E.J., Wilkinson, J.E., Avner, E.D., and Woychik, R.P. (1996). Functional correction of renal defects in a mouse model for ARPKD through expression of the cloned wild-type Tg737 cDNA. Kidney Int. *50*, 1240–1248.

Yoder, B.K., Richards, W.G., Sommardahl, C., Sweeney, W.E., Michaud, E.J., Wilkinson, J.E., Avner, E.D., and Woychik, R.P. (1997). Differential rescue of the renal and hepatic disease in an autosomal recessive polycystic kidney disease mouse mutant. A new model to study the liver lesion. Am. J. Pathol. *150*, 2231–2241.

Yoder, B.K., Richards, W.G., Sweeney, W.E., Wilkinson, J.E., Avener, E.D., and Woychik, R.P. (1995). Insertional mutagenesis and molecular analysis of a new gene associated with polycystic kidney disease. Proc. Assoc. Am. Phys. *107*, 314–323.

Yokoyama, T., Copeland, N.G., Jenkins, N.A., Montgomery, C.A., Elder, F.F., and Overbeek, P.A. (1993). Reversal of left-right asymmetry: a situs inversus mutation [see comments]. Science *260*, 679–682.